Noise reduction of UDV measurements in liquid metal experiments with high magnetic fields

Martin Seilmayer, Frank Stefani and Thomas Gundrum
Helmholtz-Zentrum Dresden-Rossendorf

The last decades have seen a number of liquid metal experiments on the interaction of magnetic fields and the flow of electrically conducting fluids. The opaqueness of liquid metals requires non-optical methods for inferring the velocity structure of the flow. Quite often, such experiments are carried out with very high electrical currents to generate the necessary magnetic fields. Depending on the specific purpose, these currents can reach several kA. The utilized switching mode power supply can then influence seriously the UDV measurements by electromagnetic interference. As an example, a recent experiment on the azimuthal magnetorotational instability (AMRI) has shown that a hydrodynamically stable Taylor-Couette flow becomes unstable under the influence of a high azimuthal magnetic field. An electrical current on the axis of the experiment with up to $20\,kA$ generates the necessary field to destabilize the flow. We will present experimental results on this AMRI experiment carried out at the PROMISE facility with an enhanced power supply. For this system, we discuss the elaborate measures that were needed to obtain a reasonable signal-to-noise ratio of the ultrasonic measurement system. In dependence on various parameter variations, some typical features of the observed instability, such as the energy content, the wavelength, and the frequency are analyzed and compared with theoretical predictions.

Keywords: Taylor-Couette flow, magnetic fields, noise reduction, UDV

1 MOTIVATION FOR THE EXPERIMENT

The classical Taylor-Couette experiment [1-2] consists of an inner and an outer cylinder with radii r_i and r_o, respectively. These concentric cylinders can rotate independently with angular frequencies $\Omega_i = 2\pi f_i$ and $\Omega_o = 2\pi f_o$. Rayleigh's criterion [3] states that the flow of a non-viscous fluid in the gap between two concentric cylinders is stable against small perturbations if the angular momentum increases outwards, i.e. if

$$\frac{\partial}{\partial r}\left(r^2\Omega(r)\right)^2 > 0. \quad (1)$$

In cylindrical coordinates $\{r, \Phi, z\}$ the ideal velocity profile of the Taylor-Couette flow has the following form:

$$v_\Phi = a_\Omega r + \frac{b_\Omega}{r}. \quad (2)$$

The parameters a_Ω and b_Ω can be determined from the ratio of the radii $\hat{\eta} = r_i/r_o$ and the ratio of the angular frequencies $\hat{\mu} = \Omega_o/\Omega_i$. The radial dependence of the angular frequency $\Omega(r)$ can then be written as

$$\Omega(r) = \Omega_i\left(\frac{\hat{\eta}^2 - \hat{\mu}}{\hat{\eta}^2 - 1} + \frac{r_i^2}{r^2}\frac{1-\hat{\mu}}{1-\hat{\eta}^2}\right). \quad (3)$$

Applying (1) to (3), Rayleigh's stability criterion can be formulated in the simple form

$$\hat{\mu} > \hat{\eta}^2. \quad (4)$$

Once the condition (4) is fulfilled in an ideal TC – flow, angular momentum increases outwards so that the pressure and centrifugal forces are in an equilibrium state which is hydrodynamically stable. For the more general setting that an azimuthal magnetic field $B_\Phi(r)$ is applied to the rotating fluid, Michael [4] and Chandrasekhar [5] had derived an extended stability criterion for axisymmetric perturbations, valid for an ideally conducting and non-viscous fluid:

$$\underbrace{\frac{1}{r^3}\frac{\partial}{\partial r}\left(r^2\Omega(r)\right)^2}_{Rayleigh} - \frac{r}{\mu_0\rho}\frac{\partial}{\partial r}\left(\left(\frac{B_\Phi(r)}{r}\right)^2\right) > 0. \quad (5)$$

In our case, with a central current producing a magnetic field $B_\Phi \propto 1/r$ in the fluid, the flow remains stable according to (5), if (4) is fulfilled. However, this does not mean that non-axisymmetric modes are also stable. Actually, the interaction of the current free azimuthal field $B_\Phi \propto 1/r$ with a hydrodynamically stable rotation law (4) can become unstable against non-axisymmetric perturbations [6]. This phenomenon is called azimuthal magnetorotational instability (AMRI). It is thought to play a key role in destabilizing accretion disks around protostars and black-holes, whose Keplerian rotation profile $v_\Phi \propto 1/\sqrt{r}$ would otherwise be hydrodynamically stable. This destabilization enables also the outward angular momentum transport and inward mass transport that is needed to explain the observed high accretion rates of central objects. While AMRI is well established in theory, the aim of our laboratory set-up is to support the theoretical models with experimental evidence.

2 EXPERIMENTAL SETUP

The experimental setup is a classical TC device with two concentric copper cylinders that can rotate independently, see Fig. 1. An electrically insulated copper rod carries a current up to $I = 20\ kA$ through the center of the cylinders. The azimuthal magnetic field in the liquid metal between the cylinders can then be approximated by

$$B_\Phi(r) = \frac{\mu_0}{2\pi}\frac{I}{r} \qquad (6)$$

which gives a maximal field strength at the inner cylinder of $B_\Phi(r_i) = 100\ mT$.

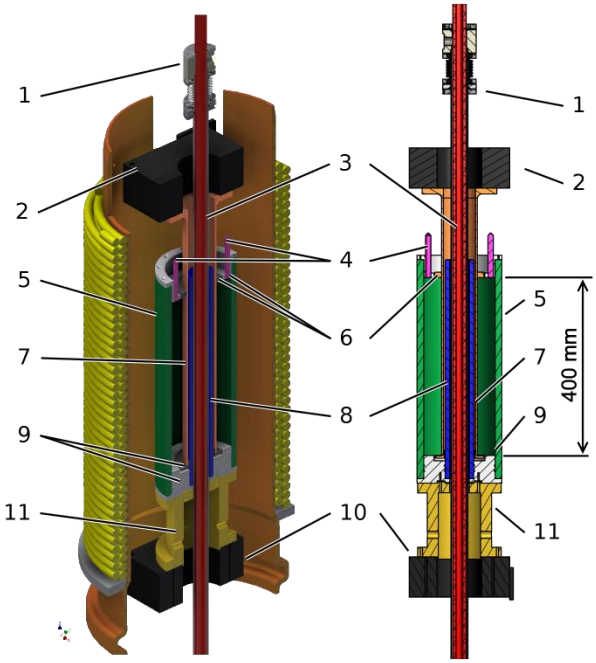

Figure 1: Sketch of the PROMISE facility. (1) Vacuum insulation; (2) Upper motor; (3) Current carrying copper rod; (4) UDV – Sensors; (5) Outer Cylinder; (6) Top Acrylic glass split rings; (7) Inner cylinder; (8) Center cylinder; (9) Bottom split rings; (10) Bottom motor; (11) Interface – Dimensions: $h = 0.4\ m$, $r_i = 40\ mm$, $r_o = 80\ mm$

The central TC unit in Fig. 1 is surrounded by an additional solenoid (yellow, only on the left panel) which can generate an axial field component B_z. For the first AMRI experiments, with a pure B_Φ-field, this axial field component is not used.

Table 1: Typical parameters for hydrodynamically stable operation of the PROMISE experiment

Parameter	Value
inner Rotation	$f_i = 0.1\ Hz$
outer Rotation	$f_o = 0.026\ Hz$
Rotation ratio	$\hat{\mu} = \Omega_a/\Omega_i = 0.26$
Geometry	$\hat{\eta} = r_i/r_a = 0.5$

The electrical conducting liquid is the eutectic alloy $Ga^{67}In^{20,5}Sn^{12,5}$ (GaInSn). This material is liquid at room temperature. The axial velocity perturbations along the height of the cylinder are measured by Ultrasound Doppler Velocimetry (UDV). A typical parameter set for the experiment is given in Table 1. The most interesting case is a stable flow which satisfies condition (4), whose destabilization by AMRI is then to be investigated.

2.1 *UDV Instrumentation*

As shown in Fig. 1, there are two $4\ MHz$ ultrasound transducers (4) installed on the top of the container. These sensors are fixed at the outer top ring, and are flush mounted at the interface to the GaInSn. The velocity component to be measured is v_z. Since the outer top ring is fixed to the outer cylinder, the sensors co-rotate with the same rotation rate Ω_o.

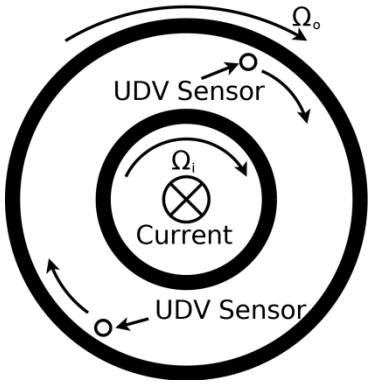

Figure 2: Schematic drawing of the sensor mounting

For the signal transmission from the frame of rotation to the laboratory frame the two UDV signals pass an ordinary slip ring below the bottom motor (Fig 1 – (10)). A DOP3010 from Signal Processing SA with modified signal lines controls the UDV sensors and calculates the two velocity profiles from each sensor. The optimized UDV parameters are listed below. The reason for choosing these numbers is discussed later on.

Table 2: Optimized ultrasound parameters

Parameter	Value
max velocity	$v_{max} = 25\ mm/s$
sound velocity GaInSn	$v_s = 2750\ m/s$
US - Frequency	$f_{UDV} \approx 3.7\ Mhz$
Pulse Repeating Frequency	$T_{PRF} \approx 7\ ms$
Number of profiles	$N_{profiles} = 150$
Resulting sampling rate	$T_s \approx 2\ s$
Number of gates	$N_{Gates} = 400$
Number of profiles per run	$n_{Profiles} = 3000$

2.2 *High magnetic field generation*

In order to identify the AMRI mode, which is a non-axisymmetric wave drifting with a frequency close to the outer cylinder rotation rate, a critical current of about $I_{crit} > 10\ kA$ is needed. By combining ten

switching mode power supplies (SMPS) of the type PE4206, an overall current up to $20\,kA$ can be provided.

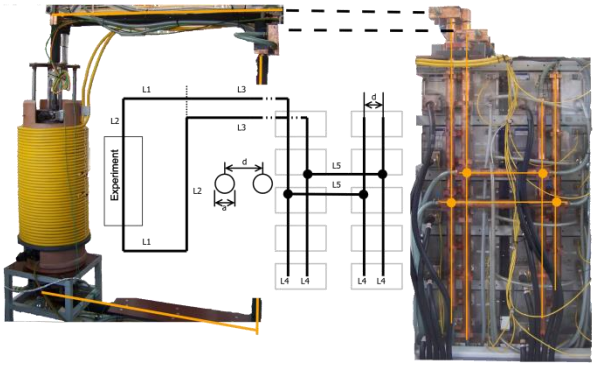

Figure 3: Modified photograph of the water cooled supply rods ($a = 30\ mm$) and power sources. Left – experimental set-up. Right – rack with ten SMPS devices.

These robust SMPS work independently from each other. This means, every single source rectifies the AC three-phase to a constant DC output without any synchronization with the neighboring power sources. This active rectification has the advantage of high efficiency, up to 85% at full load [7], but gives also a wide spectrum of electromagnetic noise.

Figure 4: Oscilloscope signals of a supply lines (SL). Top (yellow): CH1, magnetic stray field, picked up with an air coil. – Middle (purple): CH3 AC measurement of SL. – Bottom (red): Fourier transform of CH3, with a clear-cut minimum at 3.5 MHz and a peak at 4 Mhz

3 NOISE REDUCTION TO IMPROVE UDV SIGNALS

Due to parasitic capacitive and inductive coupling the electromagnetic noise originating from the SMPS propagates along the supply lines. This introduces electromagnetic distortions in the UDV signal lines. When the noise level reaches the typical voltage level of the UDV sensors $U_{UDV} = \mathcal{O}(100\,\mu V)$, the algorithm that calculates the velocities fails. The result is an unusable velocity profile, as illustrated in Fig. 5. First there is the way to reduce the noise physically by improving the installation. This is done by i) applying high current LC - low pass filters, ii) defining the reference voltage (this is necessary, since the power sources are galvanically insulated), iii) terminate each piecewise parallel line with its characteristic impedance and iv) high frequency grounding of the sources and the device frame at different locations [8]. The overall effect of all these measures is visible when comparing Fig. 6 with Fig. 5. Furthermore the UDV-frequency is changed to 3,7 MHz, i.e. the value in the minimum noise amplitude, which is given in Fig. 4.

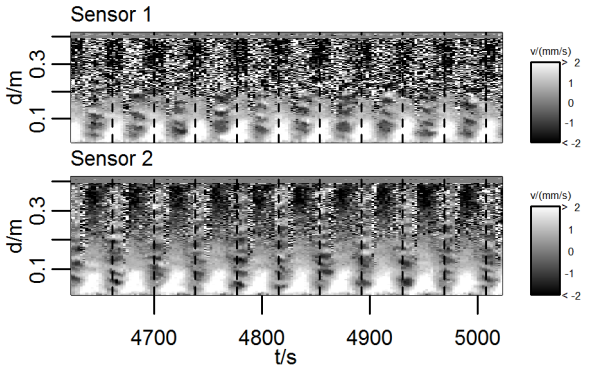

Figure 5: A segment of a velocity time series measured at $I = 18\ kA$, $\hat{\mu} = 0.26$, $f_i = 0.1\ Hz$ before the physical noise reduction was applied. Dashed lines indicate f_o, so the periodic structure appears with the same frequency.

The calculated velocities in Fig. 5 have discrete values either v_{max} or v_{min}. Summing up averages will not zero out this noise process, because the assumed model $v = v_0 + N(0,1)$ is not present at such a bad point. The work around during the preprocessing of the data is to delete these bad points and reconstruct their values.

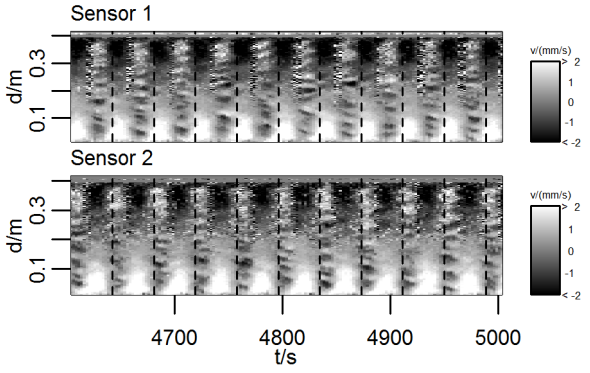

Figure 6: Same as Fig. 5 but with noise reduction at work.

For this purpose, we assume a sinusoidal model function over time for each depth with the sensor rotation frequency Ω_0. The least square estimator by Lomb-Scargle gives an estimate of the missing points for the gapped dataset [9-10]. The final step is then to filter the 2D dataset with a 2D Fourier low pass filter. The effect is to smooth out all remaining spiky events like those coming from noise. Figure 7 summarizes all these steps to illuminate the workflow. It turns out that even periodic short time events can be suppressed very well. The faulty raw data points would blow up the scale, that is why the remaining “dotted grey” line is so sparse.

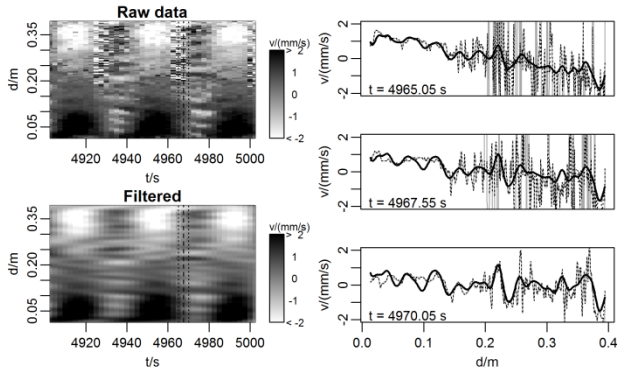

Figure 7: Segment of the time series of Fig. 6. Left side: The raw data shows distortions due a bad position on the slip ring. Right side: 3 velocity profiles with raw data (dotted), gapped data (grey); 2D FFT filtered (black)

4 SOME RESULTS

After performing physical and computational noise reduction the wave structure $\tilde{v}$ of AMRI becomes visible when the stationary flow $\overline{v}$ is subtracted:

$$\tilde{v} = v_0 - \overline{v} \tag{7}$$

With two opposing sensors available, the non-axisymmetric mode can be identified by subtracting the two datasets. Figure 8 illustrates the final non-axisymmetric wave structure as seen in the rotating frame of the sensors.

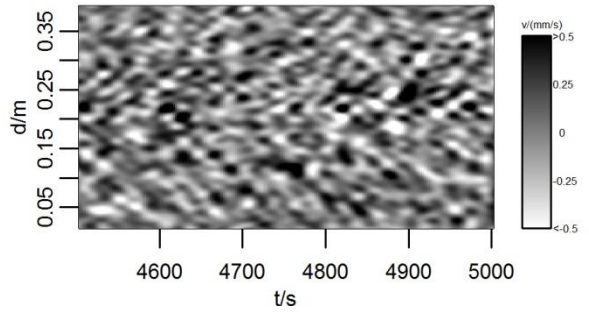

Figure 8: Wavy structure due to AMRI action; parameters are the same as in Fig. 6

5 CONCLUSION

The question of whether a hydrodynamically stable flow can be destabilized in presence of an azimuthal magnetic field is of great astrophysical importance. The PROMISE facility has been extended and improved to reduce the level of noise in the measurement data. It was shown that physical noise reduction in combination with appropriate filtering techniques leads to a reasonable data quality. Even for the largest possible current of $20\,kA$, which produces maximal noise, it is possible to get good signals until the full depth of $400\,mm$. The improvement of the signal results from combination of all applied measures. The introduction of the reference potential for each transmission line had, perhaps, the largest reduction effect on the noise. By processing the data one finally finds a clear evidence for a non-axisymmetric wave mode [11].

REFERENCES

[1] G. Taylor, "Stability of a viscous liquid contained between two rotating cylinders," *Philosophical Transactions of the Royal Society of London. Series A, Containing Papers of a Mathematical or Physical Character,* vol. 223, pp. 289--343, 1923.

[2] C. D. Andereck, S. Liu and H. L. Swinney, "Flow regimes in a circular Couette system with independently rotating cylinders," *Journal of Fluid Mechanics,* vol. 164, pp. 155--183, 1986.

[3] Rayleigh, "On the dynamics of revolving fluids," *Proceedings of the Royal Society of London Series A - Containing Papers of a Mathematical and Physical Charakter,* vol. 93, pp. 148-154, MAR 1917.

[4] D. Michael, "The stability of an incompressible electrically conducting fluid rotating about an axis when current flows parallel to the axis," *Mathematika,* vol. 1, pp. 45--50, 1954.

[5] S. Chandrasekhar, "Hydrodynamic and hydromagnetic stability," *International Series of Monographs on Physics, Oxford: Clarendon, 1961,* vol. 1, 1961.

[6] G. Rüdiger, M. Gellert and R. Hollerbach, "Astrophysical and experimental implications from the magnetorotational instability of toroidal fields," *Monthly Notices of the Royal Astronomical Society,* vol. 1, no. 438, pp. 271-277, 2014.

[7] plating electronic GmbH, "www.plating.de," [Online]. Available: power-station-pe4206-de.pdf. [Accessed 27 02 2014].

[8] Brüel & Kjaer Vibro, Allgemeine Erdungsempfehlung, Darmstadt, 2006.

[9] A. Mathias, F. Grond, R. Guardans, D. Seese, M. Canela and H. H. Diebner, "Algorithms for Spectral Analysis of Irregularly Sampled Time Series," *Journal of Statistical Software,* vol. 11, pp. 1--27, 19 5 2004.

[10] J. D. Scargle, "Studies in astronomical time series analysis. II-Statistical aspects of spectral analysis of unevenly spaced data," *The Astrophysical Journal,* vol. 263, pp. 835--853, 1982.

[11] M. Seilmayer, V. Galindo, G. Gerbeth, T. Gundrum, F. Stefani, M. Gellert, G. Rüdiger, M. Schultz and R. Hollerbach, "Experimental evidence for non-axisymmetric magnetorotational instability in an azimuthal magnetic field," *arXiv preprint arXiv:1311.7223,* 2013.